Dendritic mRNA Targeting of Jacob and N-Methyl-D-aspartate-induced Nuclear Translocation after Calpain-mediated Proteolysis[*]

Stefan Kindler[‡], Daniela C. Dieterich[§¶], Janin Schütt[‡], Jale Sahin[§1], Anna Karpova[§], Marina Mikhaylova[§], Claudia Schob[‡], Eckart D. Gundelfinger[∥], Hans-Jürgen Kreienkamp[‡], and Michael R. Kreutz[§2]

From the [‡]Institute of Human Genetics, University Medical Center Hamburg Eppendorf, 20246 Hamburg, Germany and the [§]Project Group Neuroplasticity, the [¶]Emmy Noether Research Group, and the [∥]Department of Neurochemistry/Molecular Biology, Leibniz Institute for Neurobiology, 39118 Magdeburg, Germany

Jacob is a recently identified plasticity-related protein that couples N-methyl-D-aspartate receptor activity to nuclear gene expression. An expression analysis by Northern blot and in situ hybridization shows that Jacob is almost exclusively present in brain, in particular in the cortex and the limbic system. Alternative splicing gives rise to multiple mRNA variants, all of which exhibit a prominent dendritic localization in the hippocampus. Functional analysis in primary hippocampal neurons revealed that a predominant cis-acting dendritic targeting element in the 3′-untranslated region of Jacob mRNAs is responsible for dendritic mRNA localization. In the mouse brain, Jacob transcripts are associated with both the fragile X mental retardation protein, a well described trans-acting factor regulating dendritic mRNA targeting and translation, and the kinesin family member 5C motor complex, which is known to mediate dendritic mRNA transport. Jacob is susceptible to rapid protein degradation in a Ca^{2+}- and Calpain-dependent manner, and Calpain-mediated clipping of the myristoylated N terminus of Jacob is required for its nuclear translocation after N-methyl-D-aspartate receptor activation. Our data suggest that local synthesis in dendrites may be necessary to replenish dendritic Jacob pools after truncation of the N-terminal membrane anchor and concomitant translocation of Jacob to the nucleus.

The link between excitatory neurotransmission and transcriptional and translational regulation has attracted much interest for many years because multiple processes ranging from metabolic homeostasis to learning and memory require activity-driven gene expression in neurons (1, 2). Particularly signaling from N-methyl-D-aspartate (NMDA)[3] type glutamate receptors to the nucleus has been implicated in synaptic plasticity, and some molecules have been identified that can translocate from synaptic and extrasynaptic sites to neuronal nuclei after NMDA receptor activation (3–7). In a recent study, we have identified Jacob, a protein that triggers long lasting changes in the cytoarchitecture of dendrites and the number of spine synapses in pyramidal neurons via coupling of NMDA receptor signaling to nuclear gene expression (6). Following activation of synaptic and extrasynaptic NMDA receptors, Jacob is recruited to neuronal nuclei, and this in turn results in a rapid stripping of synaptic contacts and in a drastically altered morphology of the dendritic tree (6). Nuclear import of Jacob utilizes the classical importin pathway (6, 7), and the synaptic Ca^{2+}-binding protein Caldendrin regulates the extra-nuclear localization of Jacob by competing with the binding of importin-α to a bipartite nuclear localization signal in Jacob (6). In the nucleus, Jacob can trigger dephosphorylation of the transcription factor CREB and gene expression that destabilizes synaptic contacts. These events may be part of homoeostatic plasticity, i.e. the constant optimization of synaptic input of a given neuron (6, 8). Thus, it seems likely that the balance between the nuclear and extra-nuclear pool of Jacob is highly dynamic and tightly controlled.

In the present study, we have investigated the local expression and turnover of Jacob in more detail. We identified a number of alternative splice products, all of which are largely restricted to the limbic system and cortex. In the hippocampus, all Jacob mRNAs exhibit a prominent dendritic localization, which is mediated by a dendritic targeting element (DTE) residing in the 3′-untranslated region (3′-UTR). Jacob transcripts are associated both with KIF5c, a motor implicated in cytoplasmic transport of several dendritic mRNAs, and the fragile X mental retardation protein (FMRP), which is thought to play a central role in both dendritic trafficking (9, 10) and local translation of mRNAs at postsynaptic sites (11–
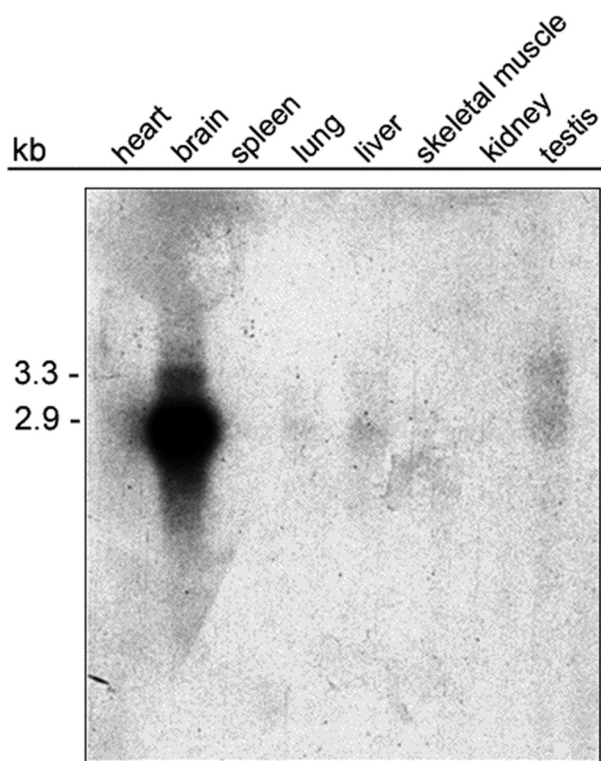
FIGURE 1. **Jacob is only abundant in brain.** A rat multiple tissue Northern blot was hybridized with a radioactive Jacob cDNA probe encompassing bp 104–2827 of the Jacob rat mRNA (accession number AJ293697). Hybridization of the blot with a Jacob cDNA probe identifies a broad band at about 3.0 kb and a weaker one at 3.6 kb in rat brain mRNA. In testis and other tissues only a very weak or no signal was observed.

14). Interestingly, Jacob is a very unstable protein that is rapidly degraded in a Ca^{2+}- and Calpain-sensitive manner. In conjunction with its dynamic translocation from dendrites to the nucleus, this might impose the necessity of replenishing the cytoplasmic protein pool by the local translation of dendritic mRNAs.

EXPERIMENTAL PROCEDURES

Analysis of Transcript Distribution—Northern blot analysis was performed with a multiple tissue Northern blot (Clontech) according to published procedures (15) using a ^{32}P-labeled cDNA sample encompassing bp 104–2827 of the Jacob cDNA. *In situ* hybridization of rat brain cryostat sections was performed as described (16). Control experiments included hybridization with a sense probe and prior RNase treatment.

Antisense Oligonucleotides—Antisense oligonucleotides were deduced from the Jacob cDNA (accession number AJ293697): 5′-CAG GGC TGG CTC TCT AGA GAT GGT GTA CAC ACG GGG CTG G-3′ (Jacob-pan); 5′-TCT CCC GTT TCC GAC GCT TCC TCT CCG CGT AGC C-3′ (Jacob+exon6); 5′-GGA GTC GTG GGA GGT GTC GGC TTT CAT AGG GGT G-3′ (Jacob+exon8); 5′-AGG TGT TTG CGG AAG TTC GAT ATG GCT TGC ATA G-3′ (Jacob-exon6); 5′-GCT CTG TAG GTC ACT GCT CTG GGC TTT CAC CCG C-3′ (Jacob-exon8); and 5′-CCC ACG ACT CCC GAG ACA CTA ATC TCC TCC AAG GTG-3′ (Jacob-exon 9). The oligonucleotide sequence for tubulin-α probe was 5′-GGA CCA GAA TAA ACA TCC CTG TGA AAG CAG CAC CTT GTG AC-3′. Corresponding sense oligonucleotides were used as controls.

Expression Vectors—Plasmids pNEu$_{2432-3071}$ and pNEtub have been previously described (11). Vectors pNEL$_{134-1603}$ and pNEL$_{1625-2827}$ are derivatives of the plasmid pNE (11) and contain nucleotides 134–1603 and 1625–2827 of the Jacob cDNA (accession number AJ293697) downstream of the EGFP coding region. *In vivo* time lapse imaging was done with a plasmid where EGFP is downstream of the coding region of Jacob (6). For bacterial protein production the first 230 amino acids (nucleotides 134–824) of Jacob were cloned into pMALC2X.

Animals, Cell Culture, Western Blotting, Immunocytochemistry, Transfection, and in Situ Hybridization Analysis—Wistar rats, Fmr1$^{-/-}$ mice (knock-out; B6.129P2-Fmr1^{tm1Cgr} strain; Jackson Laboratory) and congenic C57BL/6J wild type mice were raised in the animal facility of the
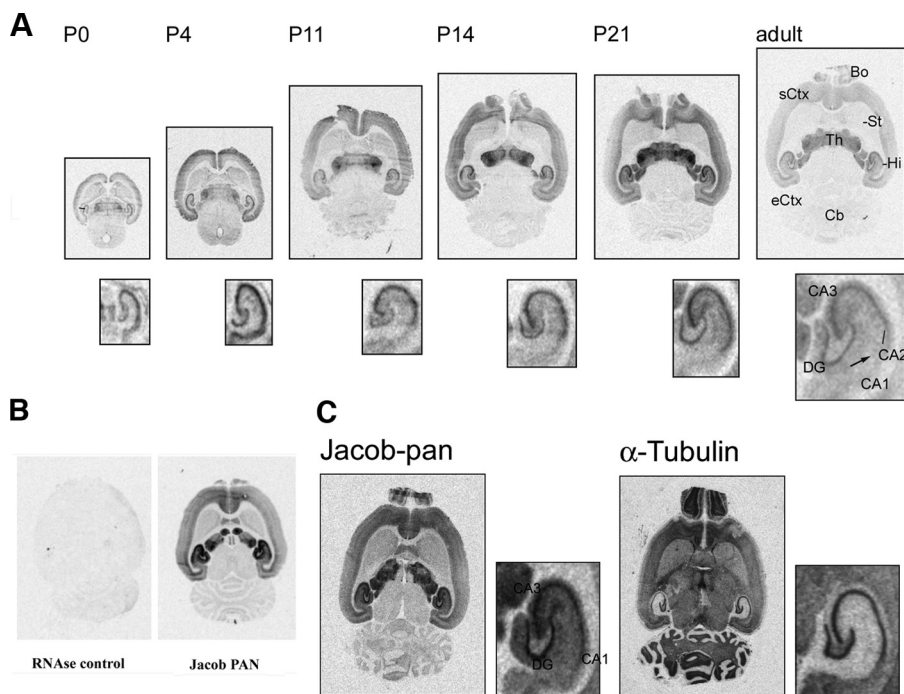

FIGURE 2. **Jacob is prominently expressed in cortex and the limbic brain and exhibits a dendritic mRNA in the hippocampus.** *A*, *in situ* hybridization of horizontal brain sections from postnatal (*P*) 0, P4, P11, P14, P21, and adult rats. X-ray film images of slices labeled with probe Jacob-pan (see "Experimental Procedures") are depicted. Magnifications of the hippocampal formation are shown in the *lower panels*. *Bo*, olfactory bulb; *sCtx*, somatosensory cortex; *Th*, thalamus; *St*, striatum; *eCtx*, entorhinal cortex; *Cb*, cerebellum; *Hi*, hippocampus; *CA1*, Ammon's horn subfield 1; *CA2*, Ammon's horn subfield 2; *CA3*, Ammon's horn subfield 3; *DG*, dentate gyrus. *B*, hybridization on sections pretreated with RNase H resulted in no signal above background. *C*, comparison of Jacob and tubulin-α hybridization signals in the hippocampus.

A

| No.	isoforms	coding exons	aa	molecular weight [kDa]	
				calculated	*in vitro* transcription/translation
1	wildtype	1-16	532	60	72
2	ΔIS (ΔExon5)	1-4 + 6-16	530	60	72
3	ΔNLS (ΔExon6)	1-5 + 7-16	509	57.3	70
4	ΔLCR1 (ΔExon8)	1-7 + 9-16	502	56.5	68
5	ΔIS/NLS (ΔExon5+6)	1-4 + 7-16	507	57	70
6	ΔNLS/LCR1 (ΔExon6+8)	1-5 + 7 + 9-16	479	53.7	65
7	ΔIS/NLS/LCR1 (ΔExon5+6+8)	1-4 + 7 + 9-16	477	53.5	65
8	ΔLCR2 (ΔExon9)	1-8 + 10-16 (frameshift leads to a stop at aa 337)	337	37.6	-
9	ΔIS/LCR1 (ΔExon5+8)	1-4 + 6-7 + 9-16	500	56.3	68
10	ΔExon5+9	1-4 + 6-8 + 10-16	335	37.4	-
11	ΔExon6+9	1-5 + 7-8 + 10-16	314	34.9	-
12	ΔExon8+9	1-7 + 10-16	307	34.1	-
13	ΔExon5+6+9	1-4 + 6-7 + 10-16	312	34.7	-
14	ΔExon5+8+9	1-4 + 6-7 + 10-16	305	33.9	-
15	ΔExon6+8+9	1-5 + 7 + 10-16	286	31.4	-
16	ΔExon5+6+8+9	1-4 + 7 + 10-16	284	31.2	-
17	LCR3	1-9 + intron9 + 10	408	45.1	-
17*	LCR3 (human)	1-9 + intron9 + 10	402	44.3	-

B

C
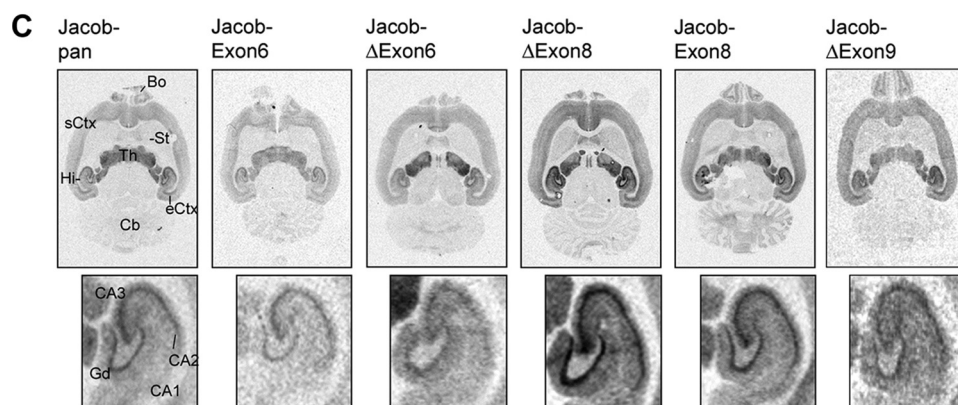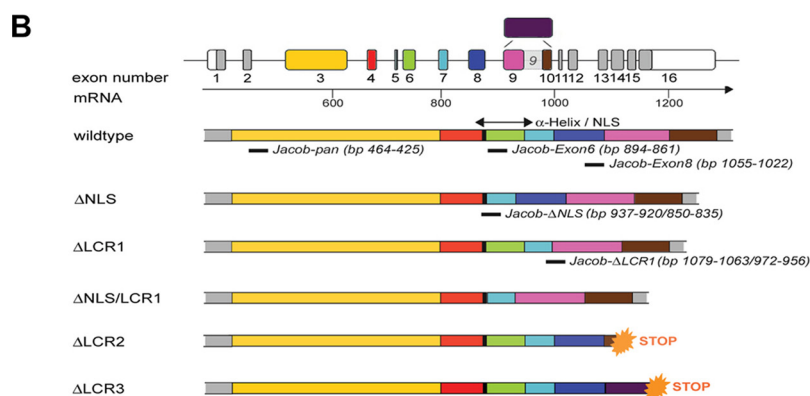
FIGURE 3. Several Jacob splice isoforms exist. *A*, confirmed (*isoforms 1–8* and *17/17**) and putative (*isoforms 9–16*) splice isoforms of Jacob. Confirmed isoforms were identified by a cDNA library screen and public data base searches. *B*, schematic illustration of the Jacob gene structure, deduced splice isoforms, and position of antisense oligonucleotides used in this study. Note that intron 9 (*opaque gray field* between exons 9 and 10) is present in isoform DLCR3, resulting in a frameshift and a STOP after amino acid 408 in the murine amino acid sequence (*isoform 17*) and after amino acid 402 in the human isoform (*isoform 17**). *C*, *in situ* hybridization of horizontal brain sections from adult rats. X-ray film images of slices labeled with probes specific for Jacob-pan and for a selection of splice-isoforms (see "Experimental Procedures") are depicted. Magnifications of the hippocampal formation are shown in the *lower panel*. *Bo*, olfactory bulb; *sCtx*, somatosensory cortex; *Th*, thalamus; *St*, striatum; *eCtx*, entorhinal cortex; *Cb*, cerebellum; *Hi*, hippocampus; *CA1*, Ammon's horn subfield 1; *CA2*, Ammon's horn subfield 2; *CA3*, Ammon's horn subfield 3; *Gd*, dentate gyrus.

ever, the neurons were grown in neurobasal medium (Invitrogen) without glial feeder layer. Rat hippocampal neurons were transfected 8 days after plating (days *in vitro* (DIV) and fixed 6 days after transfection. Immunocytochemical analysis, synthesis of digoxigenin-labeled RNA probes, *in situ* hybridization analysis, and scoring of recombinant dendritic transcripts was performed as described (17). Combined fluorescent *in situ* hybridization/immunocytochemical approaches were performed with Cy3-coupled mouse monoclonal anti-digoxigenin (Roche Applied Science) and rabbit polyclonal anti-MAP2 antibodies (generous gift from Craig C. Garner, Stanford University) and rabbit polyclonal Jacob antibodies (6) followed by Cy3-coupled sheep anti-mouse (Sigma) and Alexa-Fluor$_{488}$-coupled goat anti-rabbit antibodies (Molecular Probes-Invitrogen). Jacob RNA probes comprise full-length coding and 3'-untranslated regions. Images captured with a Zeiss Axiovert 135 microscope (Carl Zeiss Micro-Imaging) and Openlab software (Improvision) or a laser-scanning microscope (TCS-SP2 Leica) were mounted using Adobe Photoshop CS (Adobe Systems) and Freehand (Macromedia) software. For stimulation, primary hippocampal neurons (DIV16 for calpeptin and DIV21 for E64d) were incubated with 60 μM calpeptin and 50 μM E64d for 30 min at 37 °C. NMDA (100 μM) was applied for 5 min in stimulation buffer (Neurobasal medium with 7.5 μM anisomycin) either in the absence or presence of inhibitors. After stimulation, the cells were washed twice with stimulation buffer and then incubated for 30 min at 37 °C. The cells were fixed with 4% paraformaldehyde in 1× phosphate-buffered saline (150 mM NaCl, 20 mM sodium phosphate, pH 7.4) for 10 min at 37 °C and then incubated in

University Medical Center Hamburg-Eppendorf or the Leibniz Institute for Neurobiology. Primary neurons were essentially prepared and transfected as described (17). However, permeabilization solution (0.25% Triton X-100 in 1× phosphate-buffered saline) for 10 min at room temperature. Subsequently, they were incubated in blocking solution (2% bovine
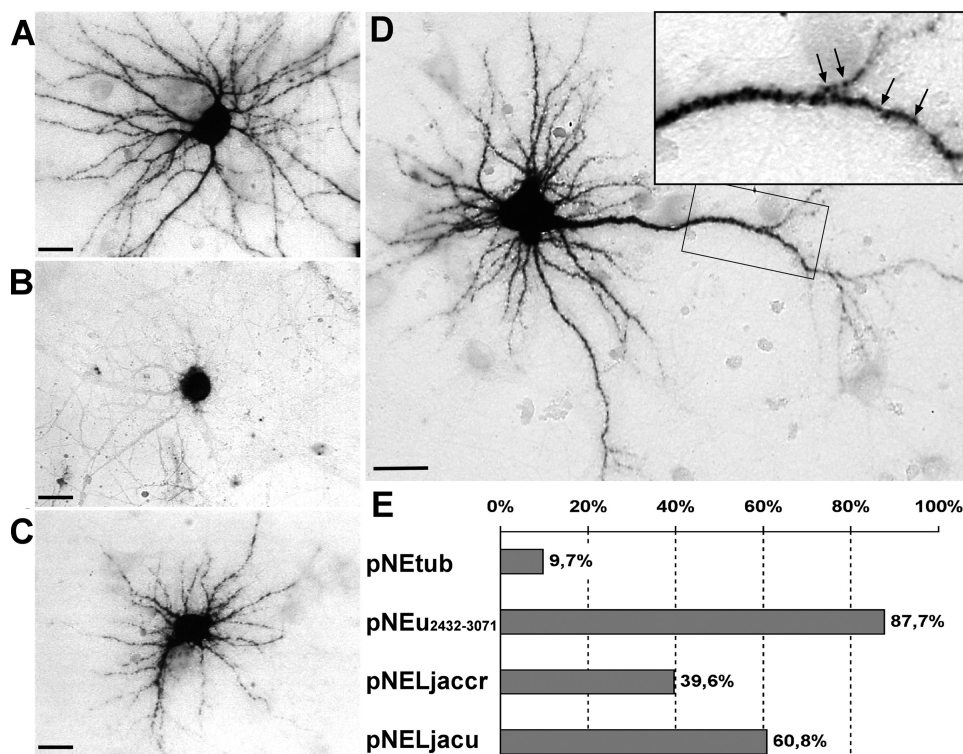
FIGURE 4. **Identification of a DTE in Jacob mRNAs.** Hippocampal neurons were transfected with the listed eukaryotic expression vectors, and the encoded recombinant mRNAs were detected by *in situ* hybridization using an antisense probe directed against the EGFP coding sequence. The *dark color* indicates the subcellular distribution of reporter mRNAs. In contrast to somatically restricted EGFP-α-tubulin transcripts (*B*), chimeric mRNAs containing the previously characterized MAP2-DTE (*A*), the coding region (*C*), or the 3′-UTR of Jacob transcripts (*D*) reside in cytoplasmic granules, which are dispersed along dendritic processes (see *inset* in *D* showing an enlarged section of a dendritic shaft). The *bar graph* in *E* indicates the percentages of primary neurons, in which reporter transcripts transcribed from the listed expression vectors are dendritically localized. *Scale bars*, 10 μm.

binding domain of mouse KIF5c (amino acid residues 826–920, accession number NP_032475) were expressed in *Escherichia coli* and purified using GSH-Sepharose (GE Biotech). GST-KIF5C-coated Sepharose beads were used to affinity purify KIF5C-associated cargos from mouse brain homogenates as described (10). Immunoprecipitation experiments were performed with antibodies directed against fragile X mental retardation protein (rabbit polyclonal antibody H-120; Santa Cruz Biotechnology, Heidelberg, Germany) and poly(A)-binding protein (PABP) (18) as well as irrelevant rabbit IgGs and brain extracts derived from adult male $Fmr1^{-/-}$ mice and congenic C57BL/6J wild type (WT) mice as described (19). From brain homogenates and immuno- and GST-precipitates, RNA was extracted using the RNeasy mini kit (Qiagen) and analyzed by RT-PCR and quantitative real time RT-PCR with a Rotor-Gene 3000 (Corbett, Wasserburg, Germany) using the QuantiTect SYBR Green RT-PCR kit (Qiagen) as described (19). The PCR conditions were according to the standard protocol of the manufacturer with an annealing temperature of 58 °C (40 cycles) and the following gene-specific primers: BC1, BC1-Fw (5′-GTT GGG GAT TTA GCT CAG TGG-3′) and BC1-Rev (5′-AGG TTG TGT GTG CCA GTT ACC-3′); glyceraldehyde-3-phosphate dehydrogenase (GAPDH), GAPDH-Fw (5′-TGG CAA AGT GGA GAT TGT TGC C-3′) and GAPDH-Rev (5′-AAG ATG GTG ATG GGC TTC CCG-3′); and SAPAP3, SAPAP3-Fw (5′-ACT ATT TGC AGG TGC CGC AAG-3′) and SAPAP3-Rev (5′-GGG CTA CCA TCT GAG TCT CC-3′). For Jacob and Arc/Arg3.1 mRNAs the appropriate QuantiTect Primer Assay was obtained from Qiagen (catalog numbers QT01077832 and QT00250684, respectively). RT-PCR products were analyzed on 2% agarose gels.

Quantitative Immunocytochemistry-Calpain-mediated Degradation of Recombinant Jacob—MBP fusion protein production was performed as described previously (20). Samples containing 5 nM MBP-Jacob or 5 nM MBP alone, 2 mM Ca^{+2} or 2 mM EGTA, and μ-Calpain (specific activity, 0.195 enzyme units; Calbiochem) were incubated in Calpain reaction buffer (1× Tris-buffered saline, pH 7.6). The reactions were brought to 20 μl and incubated at 30 °C for 10 s, 30 s, and 1 min. The reactions were terminated by the addition of 4× SDS sample buffer. MBP-Jacob protein degradation was visualized on immunoblots.

serum albumin, 2% glycine, 0.2% gelatin, 50 mM NH_4Cl) for 1.5 h at room temperature. The primary antibody (Jacob JB150) (6) was diluted 1:100 in blocking solution and incubated overnight at 4 °C. After washing (3 × 10 min in phosphate-buffered saline with 0.3% Triton X-100) the cells were incubated with AlexaFluor-coupled secondary goat anti-rabbit IgG antibody (1:1000 in blocking solution; Molecular Probes-Invitrogen) for 2 h at room temperature, washed as described above, and embedded in Mowiol (Calbiochem). Utilizing 4′,6-diamidino-2-phenylindole staining, the nuclei were identified, and nuclear Jacob levels were determined by calculating the mean pixel intensity from two or three nuclear planes. The differences between groups are described as relative deviations from the control. The nuclear membrane was excluded from the analysis. Images were taken using a Leica DMRXE microscope equipped with a Krypton-Argon-Ion laser (488/568/647 nm) and an acousto-optic-tunable filter for selection and intensity adaptation of laser lines. The images were analyzed with ImageJ software. *In vivo* time lapse imaging and transfection of hippocampal primary neurons with Jacob-EGFP was performed as described (6). Stimulation was done with 20 μM NMDA either in the presence or absence of 60 μM calpeptin. Western blotting was done as described previously (15).

Glutathione S-Transferase (GST) Pulldown, Immunoprecipitation, and Real Time Reverse Transcriptase (RT)-PCR—GST and the fusion protein GST-KIF5c containing the cargo
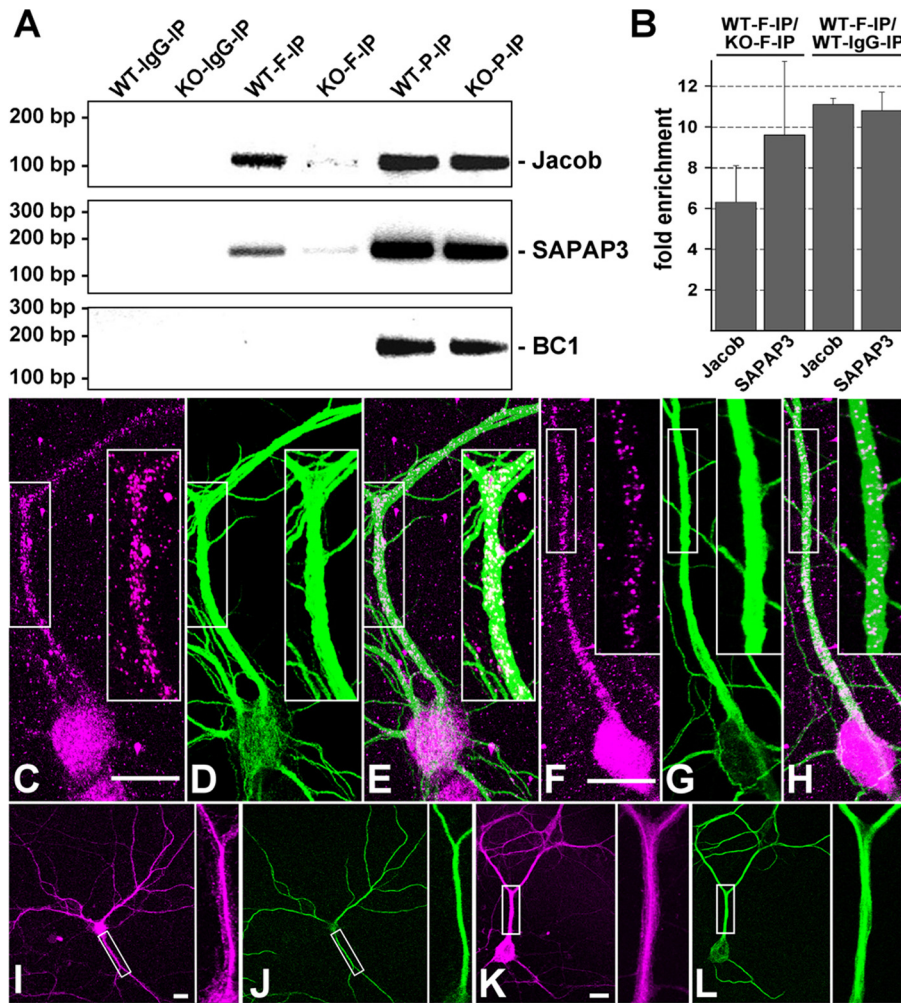
FIGURE 5. **In the mouse brain, Jacob mRNAs are associated with FMRP.** *A*, from immunoprecipitations performed with irrelevant IgGs (*IgG-IP*) or antibodies directed against FMRP (*F-IP*) and PABP (*P-IP*), respectively, and brain homogenates obtained from WT and *Fmr1*$^{-/-}$ (KO) mice. Template RNA was extracted, and RT-PCR was performed with primers specific for Jacob, SAPAP3, and BC1 RNAs. Jacob transcripts are detected in WT-F-IP and both P-IPs, but not in control IgG-IPs, and are only very faintly visible in KO-F-IP. *B*, bar graph indicating the relative amounts of Jacob and SAPAP3 mRNAs in different immunoprecipitates as evaluated by real time RT-PCR. Both Jacob and SAPAP3 transcripts are significantly enriched in WT-F-IP *versus* KO-F-IP and WT-F-IP *versus* WT-IgG-IP. *C–L*, in DIV19 primary cortical mouse neurons endogenous Jacob mRNAs (*magenta staining* in *C, E, F,* and *H*) and proteins (*magenta* in *I* and *K*) were visualized via fluorescent *in situ* hybridization and immunocytochemistry utilizing Cy3- and AlexaFluor$_{546}$-coupled goat secondary antibodies, respectively. Somatodendritic regions of neurons were identified via immunocytochemical detection of MAP2 using an AlexaFluor$_{488}$-coupled goat secondary antibody (*green*). *Insets* on the *right* of each panel display enlargements of dendritic shaft sections *boxed* in the respective panels. Jacob mRNAs and proteins exhibit similar subcellular distribution patterns in both wild type (*C–E, I,* and *J*) and FMRP-deficient mice (*F–H, K,* and *L*). Similar to the dendritically localized chimeric transcripts shown in Fig. 4, endogenous Jacob mRNAs reside in distinct granules that are dispersed along the length of MAP2-positive dendritic shafts (*insets* in *E* and *H*). Micrographs were captured with a laser-scanning microscope. *Scale bars*, 10 μm.

RESULTS

On a rat multiple tissue Northern blot two transcripts, a major one at 2.9 kb and a less intense one at 3.6 kb, can be clearly detected in the brain when hybridized with a Jacob cDNA probe. Very faint signals were detectable in the testis, and even fainter or no signals were identified in other investigated tissues (Fig. 1*A*). The two bands may reflect alternative splicing of the Jacob pre-mRNA. Subsequent *in situ* hybridization experiments revealed a strikingly restricted localization of Jacob transcripts to the limbic system and cortical areas of the rat brain. The highest levels of Jacob

mRNAs are present in the cerebral cortex, hippocampus, olfactory bulb, thalamus, and amygdala, whereas the transcript concentration in the striatum and cerebellum is very low (Fig. 2*A*). Interestingly, gene expression appears to be developmentally regulated with highest mRNA levels between the second and third postnatal week, the postnatal period during which synapto-dendritic wiring is most dynamic. The sections treated with RNase H (Fig. 2*B*) or hybridized with sense controls (data not shown) showed no signal above background. A closer inspection of the hybridization pattern revealed that Jacob mRNAs are abundantly present in the molecular layers of the hippocampus (Fig. 2, *A* and *C*), indicating dendritic localization of the transcripts. In contrast, α-tubulin transcripts are restricted to regions of neuronal somata (Fig. 2*C*).

Alternative splicing of exons 5, 6, 8, and 9 generates multiple Jacob mRNAs (Fig. 3, *A* and *B*). Thus, we sought to determine whether distinct transcripts differ in their brain distribution. Surprisingly, in the adult rat brain all tested splice variants exhibit a similar distribution pattern with slightly different levels of abundance (Fig. 3*C*). Importantly, all investigated alternatively spliced transcripts are present in the molecular layers of the hippocampus (Fig. 3*C*) and thus should be transported to dendrites. Furthermore these data suggest that the dendritic mRNA localization is due to a sequence element common to all Jacob mRNA variants. Therefore we decided to analyze the dendritic targeting of Jacob mRNAs in more detail.

Extrasomatic trafficking of mRNAs in mammalian neurons involves *cis*-acting DTEs within the localized transcripts (20–22). To determine the presence and position of DTEs within Jacob transcripts, we transfected DIV8 primary rat hippocampal neurons with eukaryotic expression vectors encoding chimeric reporter mRNAs, all of which contain the EGFP coding region as a common part, a sequence that is incapable to mediate dendritic mRNA targeting (17). Six days after transfection, the subcellular localization of recombinant transcripts was determined by nonradioactive *in situ*

hybridization with an EGFP antisense probe (17). Although reporter transcripts containing the DTE of MAP2 mRNAs displayed dendritic localization in almost 90% of the transfected cells ($n = 81$; Fig. 4, *A* and *E*), chimeric EGFP-α-tubulin transcripts were mainly restricted to somata (9,7% dendritic targeting, $n = 154$; Fig. 4, *B* and *E*). In comparison, reporter transcripts containing either the coding region (pNEL$_{jaccr}$) or the complete 3′-UTR of Jacob mRNAs (pNEL-jacu) localized to dendrites in about 40% ($n = 154$) and slightly more than 60% ($n = 250$) of the neurons, respectively (Fig. 4, *C–E*). Thus, whereas the coding region of Jacob transcripts appears to contain sequences promoting dendritic mRNA targeting, the major DTE mediating efficient extrasomatic trafficking resides in the 3′-UTR, which is common to all splice variants, in agreement with our previous observations that all Jacob transcripts are present in dendritic fields in the hippocampus. In dendrites, pNEL$_{jacu}$ derived reporter mRNAs assembled into distinct granules, which appear to resemble individual RNA transport packages (Fig. 4*D*).

FMRP is an RNA-binding protein that has been implicated in both dendritic mRNA targeting and the local control of translation at postsynaptic sites (10, 13, 23). To determine whether FMRP may be involved in cytoplasmic processing of Jacob transcripts, we probed for an *in vivo* association of the two components. Utilizing brain homogenates derived from adult male $Fmr1^{-/-}$ knock-out mice (KO) and congenic C57BL/6J WT mice as input material, we performed immunoprecipitations with FMRP-specific (F-IP) and PABP-specific (P-IP) antibodies as well as with unrelated rabbit IgGs (IgG-IP) as a control. P-IP was chosen as a positive control because PABP generally interacts with polyadenylated mRNAs. KO-F-IP and WT-IgG-IP were carried out to check for the possibility of unspecific RNA precipitation. RNA extracted from immunoprecipitates was probed for Jacob, SAPAP3, and BC1 RNAs by RT-PCR and real time RT-PCR. SAPAP3- and BC1-specific amplifications served as positive and negative controls for FMRP-associated RNAs, respectively (19, 24, 25). RT-PCR data showed that Jacob and SAPAP3 mRNAs were present in both the WT-F-IP and WT-P-IP but were basically absent or only weakly detected in the KO-F-IP and WT-IgG-IP (Fig. 5*A*). Moreover, as previously shown (19) BC1 RNA was only found in the WT-P-IP, but not in the WT-F-IP, KO-F-IP, and WT-IgG-IP (Fig. 5*A*), thus underscoring the specificity of the assay. These findings were confirmed by real time RT-PCR analysis (Fig. 5*B*). Similar to SAPAP3 mRNAs, known FMRP targets (24, 25), Jacob transcripts were found to specifically associate with FMRP (Jacob mRNA enrichment: WT-F-IP *versus* KO-F-IP = 6.3 ± 1.8 and WT-F-IP *versus* WT-IgG-IP 11.1 ± 0.3; SAPAP3 mRNA enrichment: WT-F-IP *versus* KO-F-IP = 9.6 ± 3.6 and WT-F-IP *versus* WT-IgG-IP = 10.8 ± 0.9; $n = 4$); and PABP (Jacob and SAPAP3 mRNA enrichment: WT-P-IP *versus* WT-IgG-IP = 32.4 ± 3.3 and 28.5 ± 2.1, respectively; $n = 4$). To analyze whether FMRP plays a role in dendritic targeting of Jacob mRNAs, we performed fluorescent *in situ* hybridization on cultured cortical mouse neurons. In both DIV19 wild type (Fig. 5, *C–E*) and FMRP-defi-
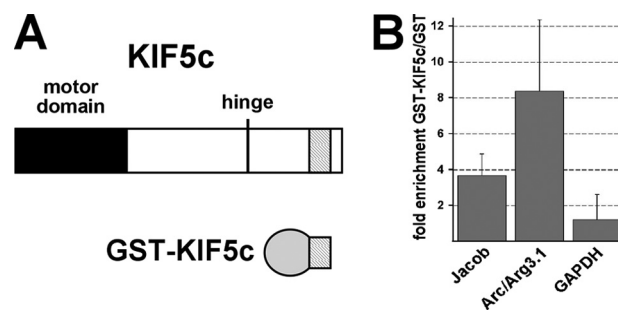
FIGURE 6. **Jacob mRNAs are part of KIF5c associated mRNA transport complexes.** *A*, schematic diagram of the motor protein KIF5c (*upper part*) indicating the motor domain (*black box*), hinge region (*thick vertical line*) and minimal binding site for the association with RNP complexes (*striped box*), as well as the GST-KIF5c fusion protein (*lower part, gray circle* indicates the GST domain). *B*, affinity chromatography was performed with cleared mouse brain lysates and GST or GST-KIF5c-coupled glutathione-Sepharose, respectively. RNA extracted from purified samples was analyzed by real time RT-PCR using specific primers for Jacob, Arc/arg3.1, and GAPDH mRNAs. The *bar graph* indicates the enrichment of a given transcript in GST-KIF5c *versus* GST-purified samples. The *simple vertical lines* specify standard deviations. The increased enrichment of Jacob and Arc/arg3.1mRNAs as compared with the GAPDH control is statistically significant ($p < 0.05$; Student's *t* test).

cient cells (Fig. 5, *F–H*), discrete Jacob mRNA granules were detected along dendritic shafts, indicating that FMRP is not an essential component of the molecular machinery that transports Jacob transcripts into dendrites. In addition, the loss of FMRP does not alter the somatodendritic localization pattern of Jacob proteins in primary neurons (Fig. 5, *I–L*).

In dendrites, mRNA granules appear to primarily move along microtubules (9, 22–25). Consistent with this notion, Kanai *et al.* (9) described ribonucleoprotein (RNP) complexes, which are associated with the cargo-binding domain of the microtubule-based motor KIF5 and contain different dendritic mRNAs, such as the Arc/Arg3.1, Ca^{2+}/calmodulin-dependent protein kinase II (αCaMKII), and Shank1 transcripts (26). To determine whether Jacob mRNAs may be transported as part of a KIF5-RNP complex, we used the minimal RNP-binding domain of KIF5c for GST pulldown experiments with mouse brain extracts (Fig. 6*A*). RNA extracted from purified samples was analyzed by real time RT-PCR. Similar to the enrichment of Arc/Arg3.1 transcripts in purified KIF5c samples as compared with GST controls (8.37 ± 3.98-fold, $n = 6$), Jacob mRNAs are also significantly enriched in the kinesin cargo sample (3.65 ± 1.22-fold, $p = 0.028$, $n = 4$) (Fig. 6*B*). In contrast, somatically restricted transcripts encoding the GAPDH are not significantly enriched in KIF5c *versus* GST samples (1.2 ± 1.4-fold, $n = 3$). Thus, among other transcripts KIF5c appears to mediate dendritic trafficking of Jacob mRNAs.

So far these data indicate that Jacob may be synthesized locally in dendrites; we hypothesized that dendritic synthesis of the protein is necessitated by the rapid dendritic turnover of the protein in response to synaptic activity. Our previous work has shown that cytoplasmic and dendritic localization of Jacob requires *N*-myristoylation and that nuclear Jacob variants are 2–3 kDa smaller as compared with cytoplasmic isoforms (6). Thus, N-terminal clipping may allow the translocation of Jacob from dendrites to the nucleus. In initial experiments we found that endogenous Jacob is particularly susceptible to degradation in a Ca^{2+}- and Calpain-dependent manner (data not
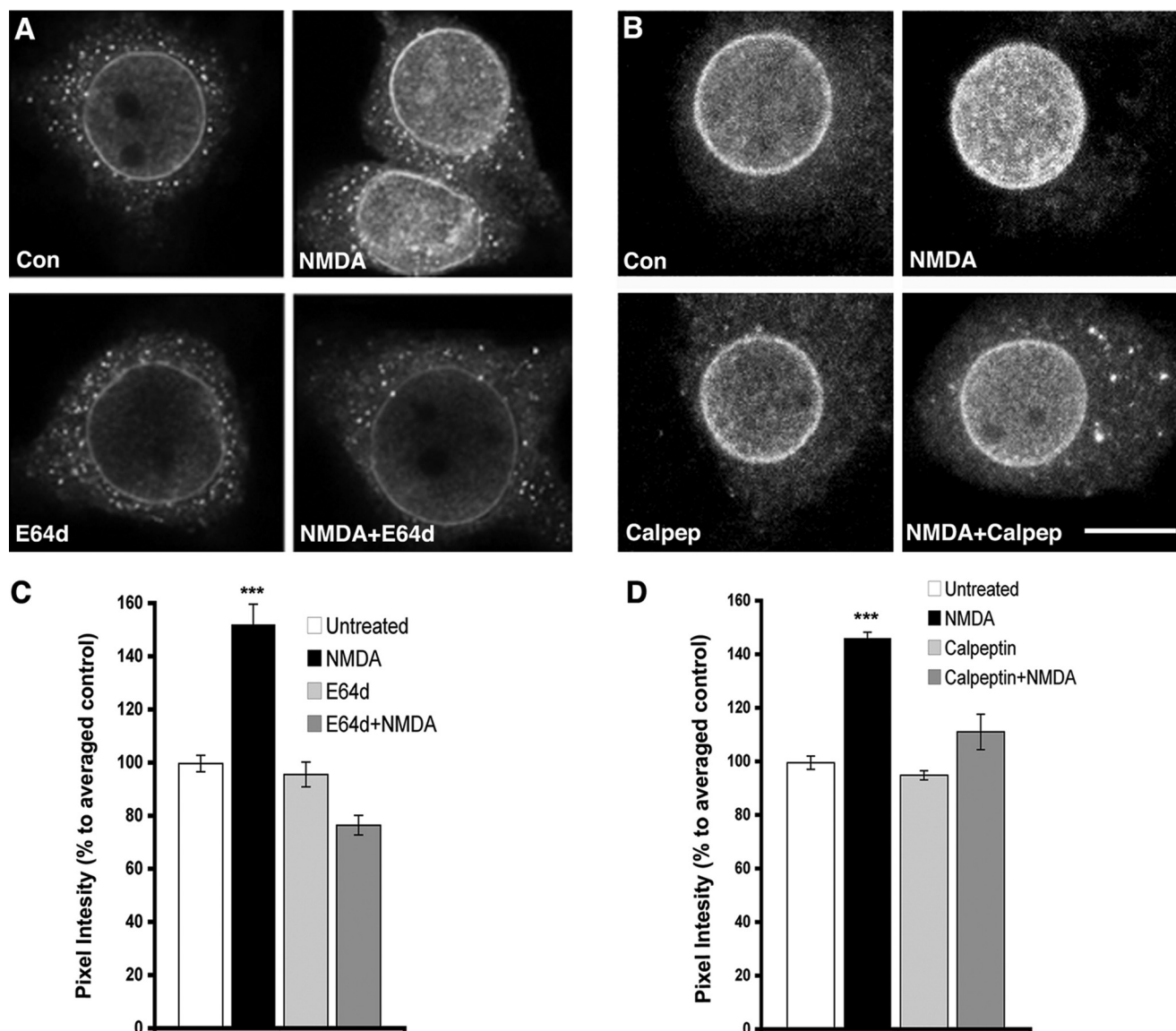
FIGURE 7. **Calpain activity is required for the nuclear translocation of Jacob.** *A* and *B*, the nuclear translocation of Jacob in primary hippocampal neurons after bath application of NMDA can be prevented by a co-application of Calpain inhibitors E64d and Calpeptin (*Calpep*). Primary cultured neurons were treated with vehicle control (*Con*), NMDA, and Calpain inhibitors as indicated. All of the experiments were done in the presence of 7.5 μM anisomycin to exclude an effect of increased *de novo* protein synthesis. Depicted are confocal images obtained from a single nuclear focal plane. The cells were stained with a Jacob antibody. The *scale bar* for *A* and *B* is 5 μm. *C* and *D*, nuclear Jacob immunofluorescence was quantified using the Image J software. N:18 for each condition in C and 20 for each condition in D. ***, $p < 0.001$.

shown). These results suggest that Jacob may indeed be particularly susceptible to activity-dependent proteolysis. We therefore analyzed whether Calpain cleavage is a prerequisite for nuclear recruitment of Jacob. As reported previously we found that after bath application of NMDA on hippocampal primary neurons, Jacob rapidly translocated within a few minutes from the cytoplasm into the nucleus (Fig. 7), a process that was completely blocked by the Calpain inhibitors calpeptin and E-64D (Fig. 7). To investigate whether calpeptin inhibits trafficking of Jacob to the nucleus from distal dendrites, we used quantitative fluorescence time lapse microscopy of hippocampal primary neurons expressing an Jacob-EGFP fusion protein. Stimulation of the cultures with NMDA led to a rapid translocation of Jacob from dendrites to the nucleus (Fig. 8). The NMDA effect could be significantly blocked if the cultures were preincubated with

calpeptin. Under this condition Jacob remained largely immobile (Fig. 8). Thus, Calpain cleavage is essential for the translocation process from dendrites to the nucleus. To finally prove that Jacob can be cleaved directly by Calpain, we purified MBP-tagged Jacob and incubated the chimeric protein with the most Ca^{2+}-sensitive Calpain isoform, μ-Calpain in the presence and absence of Ca^{2+}/EGTA. In this assay, μ-Calpain rapidly induced the Ca^{2+}-dependent clipping of Jacob close to the N terminus, leaving only a small fragment (2–3 kDa) attached to the MBP fusion part (Fig. 9). Two additional minor fragments of higher molecular weights were also visible after *in vitro* cleavage with Calpain (Fig. 9). Importantly, no cleavage of the MBP control was observed (Fig. 9), and bands for all three Calpain-cleaved fragments were either not visible or significantly attenuated in the presence of EGTA in the buffer (Fig. 9).
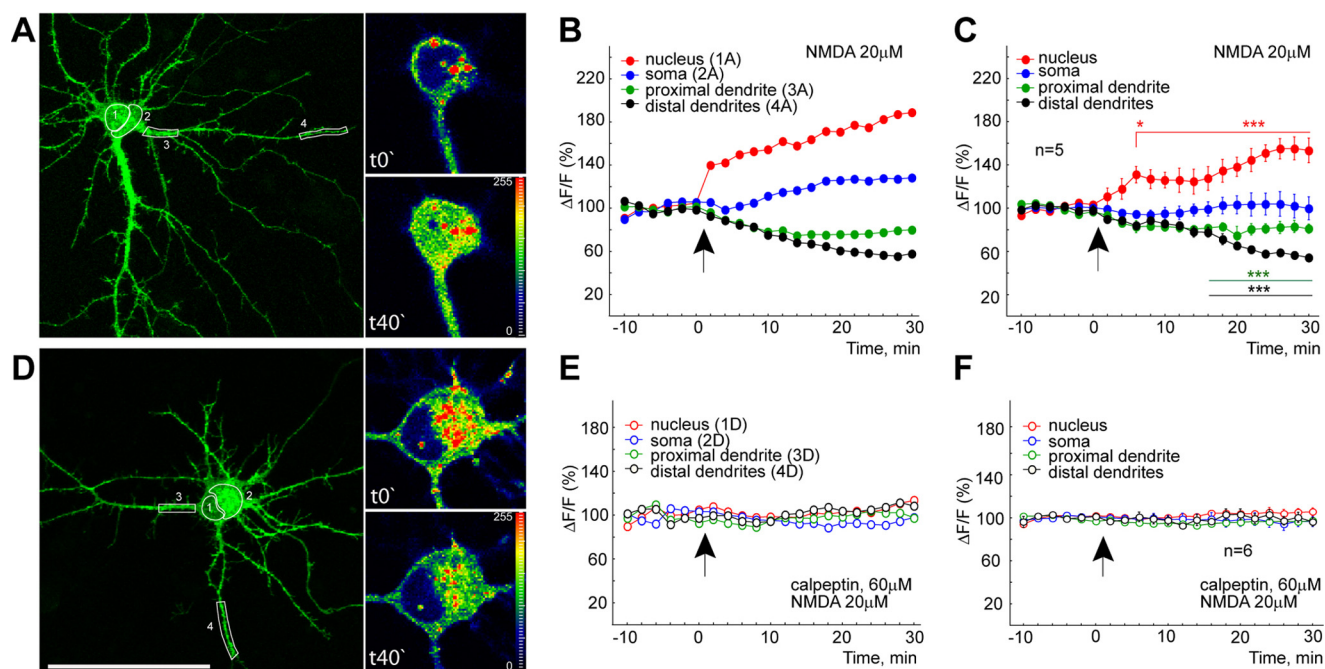
FIGURE 8. **Calpeptin attenuates Jacob translocation from distal dendrites to the nucleus after NMDA receptor stimulation.** *A* and *D*, confocal maximal intensity images of a living hippocampal primary cultured neuron (DIV10) overexpressing WT-Jacob-EGFP with correspondent representative selective confocal laserscan microscopy frames obtained from the nuclear level 10 min before (*t0′*) and 30 min after (*t40′*) stimulation with NMDA. In *D* the neuron was preincubated with calpeptin (60 μM) for 5 h. Gradient lookup tables applied to determine the dynamic range of WT-Jacob-EGFP fluorescent changes to visualize pixel intensity differences from 0 to 255 (images were not bleaching corrected) are depicted. *B* and *E*, time course of fluorescent intensity quantified using ImageJ software in depicted regions of interest before and after stimulation with NMDA (20 μM). The *arrow* indicates the time point of NMDA application. Averaged, normalized, and bleaching corrected temporal dynamics of WT-Jacob-EGFP fluorescence intensity changes after NMDA treatment with (*F*) and without (*C*) calpeptin. Without calpeptin pretreatment the increase in WT-Jacob-EGFP fluorescence in the nucleus is accompanied by a reduction of fluorescence intensity in the dendrites. Statistically significant differences in EGFP fluorescence in neuronal nuclei and dendrites after stimulation in comparison with base-line fluorescence are indicated. *, $p < 0.05$; ***, $p < 0.001$. *Scale bar*, 40 μm in *A* and *D*. All of the experiments were performed in the presence of 7.5 μM anisomycin.

DISCUSSION

Jacob was recently shown to regulate the structural integrity of synapto-dendritic regions of mammalian neurons in an NMDA receptor-dependent manner (6). In accordance with this cellular function, we show here that Jacob gene expression is essentially restricted to the limbic brain and cortex in rats, further suggesting that the protein might be involved in the dynamics of higher brain functions such as learning and memory formation that have been associated with these structures. Of note, Jacob transcripts are readily detected not only in the cell body layers of the hippocampus but also in the molecular layers, which contain the neuronal dendrites. It should be emphasized that certain mRNAs, such as those encoding ProSAP1/Shank2, translocate to dendrites only in some brain regions but not in others (27). However, we hesitate to assume that this is the case for Jacob transcripts. *In situ* hybridization signals for all Jacob splice variants were present in all layers of the cortex, and a dendritic mRNA localization was found in mouse cortical primary neurons. But it is technically difficult to assign a dendritic localization even in this laminar brain region on brain sections, whereas in brain nuclei it is almost impossible to resolve a dendritic hybridization signal.

The intensity of dendritic Jacob mRNA hybridization signals suggests an abundance comparable with other dendritic mRNAs encoding crucial postsynaptic proteins, such as the α-subunit of the αCaMKII, Arc/Arg3.1, Shank1, or SAPAP3,

which appear to have a high demand for local dendritic synthesis (26–31). Although Jacob pre-mRNA undergoes extensive alternative splicing, all splice variants appear to exhibit a similar aerial and subcellular distribution in the adult rat brain. In addition, we could establish that like in other transcripts that are translated in dendrites, a DTE is present in the Jacob-3′-UTR and that the mRNA is associated with RNA-binding and motor proteins involved in dendritic transport of RNA granules. Interestingly, a second weaker DTE also appears to be present in the coding region of Jacob, which is relatively uncommon.

Several dendritic mRNAs encode proteins that are involved in the use-dependent modification of synapses (21, 22). Because dendritic translation is regulated by neuronal activity, it is tacitly assumed that proteins, which are synthesized in dendrites, directly contribute to synaptic plasticity as well as learning and memory (21, 22). Evidence for this hypothesis has been presented for a number of dendritically localized mRNAs including those encoding αCaMKII (29), α-amino-3-hydroxy-5-methyl-4-isoxazole propionate receptors (32), and others (21, 22). At present it is unclear how the local synthesis of Jacob is regulated in dendrites. Our data suggest an *in vivo* association of Jacob mRNAs with FMRP, which acts as a *trans*-factor in the regulation of translation and dendritic mRNA targeting (10, 13, 23). However, we show herein that the neuronal loss of FMRP does not alter the somatodendritic localization of Jacob transcripts and proteins. Moreover, we also found an *in vivo* asso-
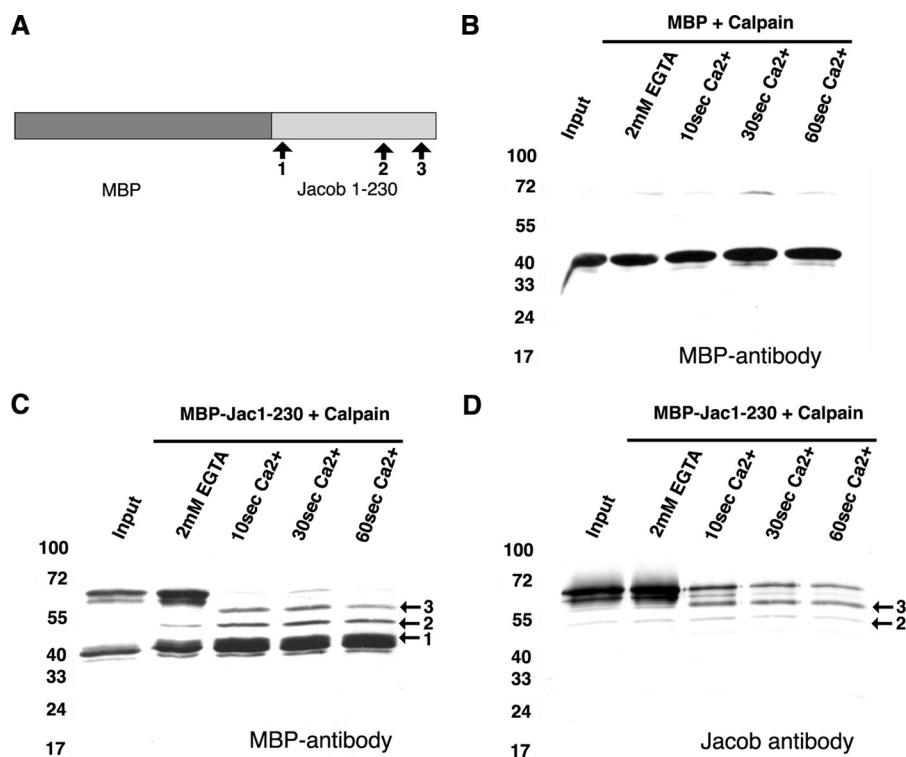
FIGURE 9. ***In vitro*** **Calpain cleavage using recombinant Jacob consisting of its first 230 amino acids and an MBP-tag.** *A*, A MBP-Jacob fusion protein covering the first 230 amino acids of Jacob was used. The region for the three potential Calpain cleavage sites as evidenced by the *in vitro* Calpain assay is depicted with *arrows*. *B*, the MBP fusion protein is not cleaved by Calpain under any of the conditions tested. The blot was processed with an MBP antibody. *C*, MBP-Jacob is rapidly cleaved after adding Calpain to the cleavage buffer. Three degradation products are readily visible within a few seconds when immunoblots were probed with an MBP antibody (see *arrows*). *D*, two of these bands are also visible when immunoblots were probed with a Jacob specific antibody. The smaller fragment (approximately the first 2–3 kDa of the Jacob fusion part), however, is not visible, possibly because it does not contain enough Jacob sequence to be detected by the polyclonal antibody. Please note that in *C* and *D* different blots had to be used because both the MBP and the Jacob antibody were raised in rabbit.

nous Jacob and that Calpain can cut off a short N-terminal domain from Jacob, making the rest of the protein accessible to nuclear import. We found previously that *N*-myristoylation is a prerequisite for the extranuclear localization of Jacob (6). Our *in vivo* studies show that Calpain inhibition completely abolishes the NMDA receptor-mediated nuclear import of Jacob. It is therefore tempting to speculate that truncation of the myristoylated N terminus by Calpain releases Jacob from membranes and enables its retrograde transport and nuclear import. Taken together, these data are in favor of an irreversible removal of the N terminus from Jacob prior to its mobilization from dendrites. This translocation event may therefore impose the necessity of replenishing the dendritic protein pool. This in consequence induces a high protein turnover and plausibly a demand for a local extrasomatic synthesis of Jacob from dendritically localized mRNAs at sites where the protein was mobilized. Because most proteins that are synthesized in dendrites are assumed to be recruited to postsynaptic sites to directly modulate synaptic function, the scenario outlined for Jacob adds a new cellular function to dendritic mRNA translation in the context of activity-dependent gene expression, and it will be fascinating to test this hypothesis.

ciation of Jacob mRNAs with RNP complexes associated with the cargo domain of KIF5c. This is interesting because these RNP particles may contain other dendritic transcripts such as αCaMKII and Arc/Arg3.1 mRNAs (9), and FMRP was also identified in the same RNP complex (9). Previous studies have shown that the activation of metabotropic glutamate receptors and brain-derived neurotrophic factor signaling is instrumental for the translation of these dendritic mRNAs (21, 22), and it is therefore conceivable that glutamatergic and brain-derived neurotrophic factor neurotransmission will also replenish the local Jacob pool. On the other hand NMDA receptor activation is both sufficient and mandatory for nuclear translocation of Jacob (6). Thus, it will be interesting to elucidate in the future whether the same stimuli that induce the nuclear translocation of Jacob are also necessary for the dendritic synthesis of the protein.

What could impose the necessity of replenishing the local pool of Jacob via translation from a dendritic mRNA? The latter argument points to a potentially important functional difference for the local dendritic synthesis of Jacob. We could show in the present study that Jacob is conspicuously sensitive to Calpain-mediated proteolysis and that Calpain activity is a prerequisite for its NMDA receptor-induced nuclear translocation from dendrites. *In vitro* experiments suggest that elevated calcium levels induce Calpain-mediated proteolysis of endoge-

REFERENCES

1. Deisseroth, K., Mermelstein, P. G., Xia, H., and Tsien, R. W. (2003) *Curr. Opin. Neurobiol.* **13,** 354–365
2. Flavell, S. W., and Greenberg, M. E. (2008) *Annu. Rev. Neurosci.* **31,** 563–590
3. Lai, K. O., Zhao, Y., Ch'ng, T. H., and Martin, K. C. (2008) *Proc. Natl. Acad. Sci. U.S.A.* **105,** 17175–17180
4. Proepper, C., Johannsen, S., Liebau, S., Dahl, J., Vaida, B., Bockmann, J., Kreutz, M. R., Gundelfinger, E. D., and Boeckers, T. M. (2007) *EMBO J.* **26,** 1397–1409
5. Jordan, B. A., Fernholz, B. D., Khatri, L., and Ziff, E. B. (2007) *Nat. Neurosci.* **10,** 427–435
6. Dieterich, D. C., Karpova, A., Mikhaylova, M., Zdobnova, I., König, I., Landwehr, M., Kreutz, M., Smalla, K. H., Richter, K., Landgraf, P., Reissner, C., Boeckers, T. M., Zuschratter, W., Spilker, C., Seidenbecher, C. I., Garner, C. C., Gundelfinger, E. D., and Kreutz, M. R. (2008) *PLoS Biol* **6,** e34
7. Jordan, B. A., and Kreutz, M. R. (2009) *Trends in Neurosci.* **32,** 392–401
8. Turrigiano, G. G. (2008) *Cell* **135,** 422–435

9. Kanai, Y., Dohmae, N., and Hirokawa, N. (2004) *Neuron* **43,** 513–525
10. Dictenberg, J. B., Swanger, S. A., Antar, L. N., Singer, R. H., and Bassell, G. J. (2008) *Dev. Cell* **14,** 926–939
11. Grossman, A. W., Aldridge, G. M., Weiler, I. J., and Greenough, W. T. (2006) *J Neurosci.* **26,** 7151–7155
12. Garber, K. B., Visootsak, J., and Warren, S. T. (2008) *Eur. J. Hum. Genet.* **16,** 666–672
13. Bardoni, B., Davidovic, L., Bensaid, M., and Khandjian, E. W. (2006) *Expert Rev. Mol. Med.* **8,** 1–16
14. Ronesi, J. A., and Huber, K. M. (2008) *Sci. Signal.* **1,** pe6
15. Seidenbecher, C. I., Langnaese, K., Sanmartí-Vila, L., Boeckers, T. M., Smalla, K. H., Sabel, B. A., Garner, C. C., Gundelfinger, E. D., and Kreutz, M. R. (1998) *J. Biol. Chem.* **273,** 21324–21331
16. Laube, G., Seidenbecher, C. I., Richter, K., Dieterich, D. C., Hoffmann, B., Landwehr, M., Smalla, K. H., Winter, C., Böckers, T. M., Wolf, G., Gundelfinger, E. D., and Kreutz, M. R. (2002) *Mol. Cell Neurosci.* **19,** 459–475
17. Blichenberg, A., Schwanke, B., Rehbein, M., Garner, C. C., Richter, D., and Kindler, S. (1999) *J. Neurosci.* **19,** 8818–8829
18. Brendel, C., Rehbein, M., Kreienkamp, H. J., Buck, F., Richter, D., and Kindler, S. (2004) *Biochem. J.* **384,** 239–246
19. Iacoangeli, A., Rozhdestvensky, T. S., Dolzhanskaya, N., Tournier, B., Schütt, J., Brosius, J., Denman, R. B., Khandjian, E. W., Kindler, S., and Tiedge, H. (2008) *Proc. Natl. Acad. Sci. U.S.A.* **105,** 734–739
20. Landgraf, P., Wahle, P., Pape, H. C., Gundelfinger, E. D., and Kreutz, M. R. (2008) *J. Biol. Chem.* **283,** 25036–25045
21. Bramham, C. R., and Wells, D. G. (2007) *Nat. Rev. Neurosci.* **8,** 776–789
22. Kindler, S., Wang, H., Richter, D., and Tiedge, H. (2005) *Annu. Rev. Cell Dev. Biol.* **21,** 223–245
23. Darnell, J. C., Mostovetsky, O., and Darnell, R. B. (2005) *Genes Brain Behav.* **4,** 341–349
24. Narayanan, U., Nalavadi, V., Nakamoto, M., Thomas, G., Ceman, S., Bassell, G. J., and Warren, S. T. (2008) *J. Biol. Chem.* **283,** 18478–18482
25. Brown, V., Jin, P., Ceman, S., Darnell, J. C., O'Donnell, W. T., Tenenbaum, S. A., Jin, X., Feng, Y., Wilkinson, K. D., Keene, J. D., Darnell, R. B., and Warren, S. T. (2001) *Cell* **107,** 477–487
26. Falley, K., Schütt, J., Iglauer, P., Menke, K., Maas, C., Kneussel, M., Kindler, S., Wouters, F. S., Richter, D., and Kreienkamp, H. J. (2009) *Traffic* **10,** 844–857
27. Böckers, T. M., Segger-Junius, M., Iglauer, P., Bockmann, J., Gundelfinger, E. D., Kreutz, M. R., Richter, D., Kindler, S., and Kreienkamp, H. J. (2004) *Mol. Cell Neurosci.* **26,** 182–190
28. Kindler, S., Rehbein, M., Classen, B., Richter, D., and Böckers, T. M. (2004) *Brain Res. Mol. Brain Res.* **126,** 14–21
29. Lyford, G. L., Yamagata, K., Kaufmann, W. E., Barnes, C. A., Sanders, L. K., Copeland, N. G., Gilbert, D. J., Jenkins, N. A., Lanahan, A. A., and Worley, P. F. (1995) *Neuron* **14,** 433–445
30. Link, W., Konietzko, U., Kauselmann, G., Krug, M., Schwanke, B., Frey, U., and Kuhl, D. (1995) *Proc. Natl. Acad. Sci. U.S.A.* **92,** 5734–5738
31. Miller, S., Yasuda, M., Coats, J. K., Jones, Y., Martone, M. E., and Mayford, M. (2002) *Neuron* **36,** 507–519
32. Ju, W., Morishita, W., Tsui, J., Gaietta, G., Deerinck, T. J., Adams, S. R., Garner, C. C., Tsien, R. Y., Ellisman, M. H., and Malenka, R. C. (2004) *Nat. Neurosci.* **7,** 244–253